Informatics and Control Problems 44 Issue 1 (2024)
journal homepage: www.icp.az

Development of the controller module of the intelligent MESSDOSE dynamograph

Y.G. Aliyev

Institute of Control Systems, Baku, Azerbaijan

ARTICLE INFO

Article history:
Received 10.04.2023
Received in revised form 17.04.2023
Accepted 25.04.2023
Available online 03.07.2024

Keywords:
Oil production
Sucker rod pump
Rod string
Polished rod
Force sensor
Dynamometry
Dynamograph
Dynamometer chart
Messdose
Microcontroller
Alternative energy source
Solar panel
Charging unit
Accelerometer
Inertial Measurement Sensors
LCD Screen
Keypad
I2C/SPI interface

ABSTRACT

Sucker rod pumping units (SRPU) are the most commonly used oil production equipment. Proper selection of the operating modes of a SRPU unit has a major impact on oil production. The correct operating modes are selected by examining the closed curves expressing the load on the hanger of the rod of the sucker-rod pump during the movement of the polished rod, i.e., the dynamometer charts of SRPU. In addition to determining the forces on the rod string, dynamometry also makes it possible to identify various malfunctions in the operation of the deep-well pump, to see how the pump works in the well. For this, it is necessary to compare the dynamometer chart obtained by means of various load cells currently used in oil wells (analog and frequency load cells, MESSDOSE load cell, etc.) with typical dynamometer charts. This article describes the hardware component of an Intelligent Messdose Dynamograph (IMD) device that can be easily installed between the crossheads of a sucker rod pumping unit and the development of a dynamograph controller (DC). The issues of building a perfect measuring device, IMD, by placing the traditional MESSDOSE dynamograph with a standard pressure sensor with DC based on modern microprocessor, communication and measurement devices in a single housing and its uninterrupted power supply from an alternative energy source are considered.

1. Introduction

Sucker rod pumping units (SRPU) are the most common pumping equipment used in oil wells. The main reason for the widespread use of SRPU is, apart from its relatively simple structure, the convenience of their use in the operation of low-flow and medium-flow rate wells [1].

In order to ensure the established technological mode of operation of the well and the deep-well pumping unit and to detect the reasons for deviations from this mode, production should be regularly monitored by measuring the amount of fluid, gas and sand pumped by the pump with group metering devices on a scheduled basis.

Based on the flow rate measurements and the calculated efficiency coefficients of the deep-well pump, it is possible to make an opinion about the correctness of the technological mode of the

E-mail address: aliyevyaver@gmail.com (Y.G. Aliyev)

www.icp.az/2024/1-09.pdf https://doi.org/10.54381/icp.2024.1.09

well, or to detect malfunctions in the operation of the pump.

One of the main methods of examining the operating mode of the pump is to study the dynamometer charts of the wells. Using a dynamometer chart, one can study: the movement of the plunger and the polished rod, the load and the force on the polished rod, the work of the force acting on the polished rod, the fluid leakage from the intake and discharge valves, as well as the gap between the plunger and the cylinder, the breakage of the rods, the effect of the gas on the pump, etc. [2, 3].

The main equipment in the automation of wells operated by SRPUs is load cells and the device that records their output data, as load cells allow obtaining the necessary data to analyze the operating modes and malfunctions of the deep-well pumping units.

Dynamometry data is obtained mainly through displacement and force sensors.

Displacement sensors determines the movement parameters of the rod string: it shows the length of travel of the suspension point of the string consisting of pump rods, the period of rotation and the moments when the rod passes through the lower and upper dead points.

Force sensor determines the parameters of the total load acting on the polished rod: it shows the total load, which is the sum of the fluid lifted from the well and the weight of the pump rod, plus the frictional forces of the pump and the string.

The use of the most modern applications of tensometry, microelectronics, mathematical processing, metrology, reliability in the creation of load cells that allow determining the output of oil wells operated by SRPUs is one of the most important and complex issues that require a complex solution approach.

These sensors, used in wells operated by SRPU, must withstand the effects of moisture, sulfur, and other destructive factors in a wide range of temperatures for a long time, must be resistant to overloading, and must operate in hazardous areas [4].

Various types of force sensors have been created for use in SRPU wells, which differ in the location and method of installation [5].

2. Problem statement

Analysis of dynamometer charts shows that the most critical and important factor in analyzing the operation modes and malfunctions of deep-well pumping units is the creation of force sensors, because there are very strict requirements, such as sensitivity, reliability, precision, simple design and ease of installation, that must be met.

The traditional MESSDOSE load cell with a tensometric MD-10 pressure sensor has been modernized by placing a modern microcontroller (MC) module in a single housing and provides only the transmission of information from the force sensor [6]. Other displacement data, which is important for building a dynamometer chart, is obtained from the displacement sensor installed on the arm of the beam. Such a structure creates considerable complexity and inaccuracy in obtaining data.

In this article, we consider creating a new dynamograph device based on the modernized MESSDOSE load cell and the development of its controller module. The requirements are as follows: in the new device, in addition to using a standard output pressure sensor (DC5V-1/8NPT) instead of the tensometric MD-10 sensor as a MESSDOSE load cell, in the same housing, displacement and temperature (inertial) measurement sensors, a radio frequency channel, an internal calibration function, a liquid crystal display and a keypad should be used. The device should be easy to install and replace, resistant to electromagnetic influences, powered by an alternative source (solar panel) and cheap.

DC5V-1/8NPT, MPU-6050 displacement and temperature sensors, STM32 microcontroller (MC), radio frequency transmitter (RF), LCD display with I2C interface and keypad (KP), power supply and charging unit (PSCU) connected to a solar panel (SP), mounted in the same housing as the traditional MESSDOSE (GDM-3), allows the device to function as a fully independent dynamograph. Therefore, the new device is called an intelligent messdose dynamograph (IMD).

In the new device, it is proposed to use a DC5V-1/8NPT pressure gauge with a connecting cable contact and protective housing as a force sensor instead of the traditional DUI with a non-standard output and low measurement accuracy, and MPU-6050 accelerometer sensors that measures direction of movement accurately as a displacement sensor instead of the inaccurate DUP.

The overall block diagram of the IMD is given in Fig. 1.

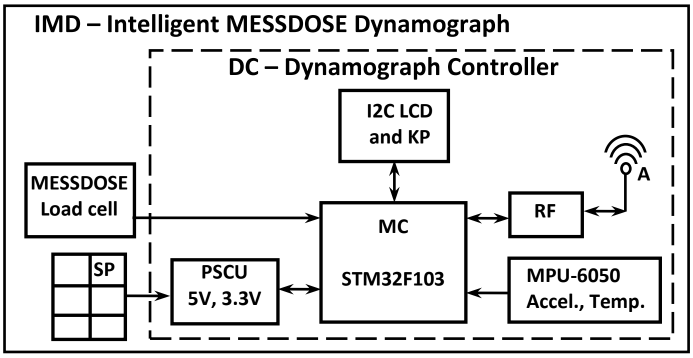

Fig. 1. Overall block diagram of the Intelligent MESSDOSE Dynamograph

3. Solution

The currently manufactured GDM-3 MESSDOSE hydraulic dynamograph allows measuring force within a range of 40kN, 80kN and 100kN in wells operated by SRPU. The dynamograph is horseshoe-shaped and can be easily installed between the crossheads of the SRPU [7]. The tension force of the rod column is brought to measure the liquid pressure in the "MESDOZ" dynamograph. A pressure sensor is installed in the MESSDOSE dynamograph and the fluid pressure is measured [5, 6].

Integration of MC, RF, MPU-6050, LCD-KP with "MESSDOSE" DC and DC5V-1/8NPT force sensor in a single housing brings new consumer qualities to IMD:

1. Since the force (pressure) and displacement (acceleration) sensors are in the same housing as the DC, there is no need for a long cable connection, electromagnetic effects disappear, measurement errors are reduced;

2. Since the short-distance measurements are made quickly, the dynamometry results are more accurate;

3. Information is transmitted to the control unit via RF channel;

4. Sufficient amount of memory makes it possible to provide complete dynamometry data both point-by-point during the real travel and during the swing period by collecting all the points in an array;

5. The presence of a temperature sensor allows to adjust the measurement results according to temperature changes;

6. Due to the display and keypad, no additional device is needed during calibration;

7. Placement of all components of the device in a single housing leads to simplification of the electrical circuit and increase in reliability;

8. Since it requires little energy, it can be fed from alternative sources (AB – accumulator battery, SP – solar panel).

The wide application of MC leads to an increase in the technical and economic indicators of industrial devices (cost, energy consumption, overall dimensions are reduced, while reliability, accuracy, speed, sensitivity are increased). At the same time, it gives them new consumer qualities (extended functionality, upgradeability, adaptability, integration, etc.). Therefore, in order to simplify the electric circuit of the IMD, to increase its reliability and ensure its flexibility, it is proposed to create it on the basis of a single MC chip (single-crystal chip).

Placement of the DC with MESSDOSE, force and acceleration sensors in a single housing is proposed as shown in Fig. 2.

The successful operation of the IMD mainly depends on the correct MC selection.

To solve this problem, a number of single-crystal chips with 8-bit MCS-51 (**m**icro **c**omputer **s**ystem), RISC (**r**educed **i**nstruction **s**et **c**ommand), 8/16- bit AVR (**a**dvanced **v**irtual **R**ISC), 16/32-bit ARM7 (**a**dvanced **R**ISC **m**achine) and 32-bit ARM-Cortex-M3/M4 (**Cortex** – stands for cerebral cortex and is understood here as the multiple layers of the cerebral cortex responsible for planning, controlling and executing actions) cores were comparatively analyzed, their structures, operating systems were studied, and the comparison of respective parameters is given in Table 1.

As can be seen from Table 1, as a result of the analysis of MC characteristics and architecture, STM32-type MCs show the best result. Although STM32F407 has the highest result, taking into account the requirements for solving the problem, the STM32F103C8T6-BP controller module with Cortex-M3 core, which is more compact, has small dimensions and sufficient technical capabilities, has been selected [8, 9].

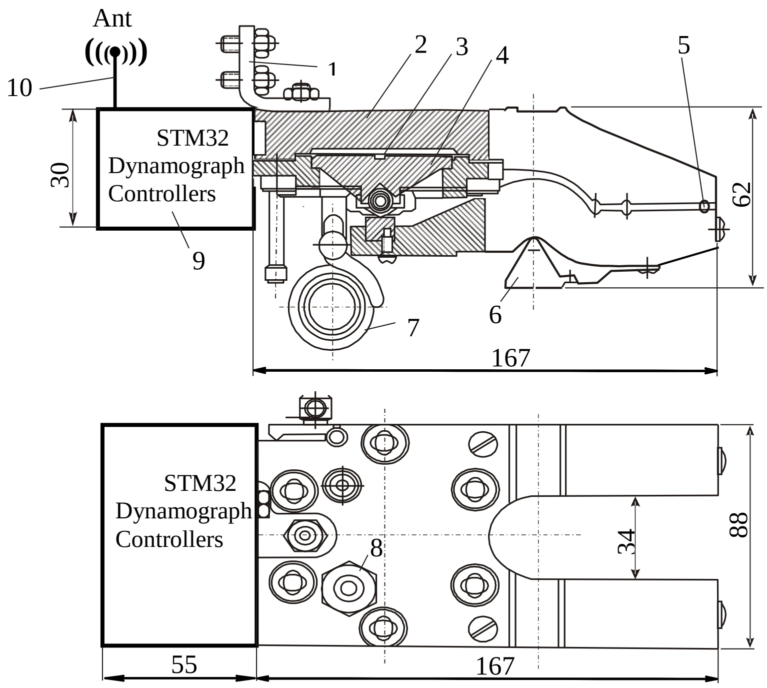

Fig. 2. Intelligent MESSDOSE dynamograph

1 – connecting curve; 2 – upper arm; 3 – membrane; 4 – beam; 5 – support roller;
6 – prism; 7 – feeding roller; 8 – pressure sensor; 9 – microcontroller; 10 – antenna

As can be seen, the traditional MESSDOSE load cell with a DC5V1/8NPT pressure sensor and other parts of the IMD device, such as STM32F103-BP module, MPU-6050 IMS (**i**nertial **m**easurement **s**ensors) acceleration, compass and temperature sensors, LCD-KP (**l**iquid **c**rystal **d**isplay panel and **k**ey**p**ad), RF (**r**adio **f**requency) radio frequency module, the power supply and the charging unit (PS-CU) connected to the accumulator battery (AB) powered by alternative energy source, solar panel (SP), are structurally and electrically placed in a single housing.

Table 1
Comparison of microprocessors

Parameters	Microprocessor type					
	STM32F407 EVK	STM32F103 C8T6-BP	LPC2148 STAMP	ATmega 32-16	ATmega 128RF1	AT89S 8253
Controller core type	CortexM4	CortexM3	ARM7	AVR	AVR	MCS-51
Register and rate of memory	32-bit	32-bit	16/32-bit	8/16-bit	8/16-bit	8-bit
FLASH program memory	1024 KB	64 KB	512 KB	32 KB	128 KB	12 KB
EEPROM storage memory	1GB (NAND)	-	32 KB	1 KB	4 KB	2 KB
RAM operating memory	192 KB	20 KB	40 KB	2 KB	16 KB	256 B
USB 2.0 interface	1	1	1	-	-	-
UART interface	4	3	2	1	2	1
SPI interface	3	2	1	1	1	1
I2C interface	3	2	2	-	1	-
SSP interface	1	-	1	-	1	-
SWD/JTAG interface	1	1	1	1	1	-
DCMI parallel camera interface	1	-	-	-	-	-
FSMC parallel NAND, LCD interface	1	-	-	-	-	-
CAN interface	2	1	-	-	-	-
SDIO interface	1	-	-	-	-	-
ETH interface	1	-	-	-	-	-
ADC (analog-to-digital converter)	24 (12-bit)	10 (12-bit)	14 (10-bit)	8 (10-bit)	8 (10-bit)	-
ADC conversion time	0.5 μs	1μs	2.5 μs	65 μs	65 μs	-
DAC (digital to analog converter)	2 (12-bit)	-	1 (10-bit)	-	-	-
RTC (real time counter)	1	1	1	1	1	-
TIM Number of Timers	17	3	2	3	2	2
Maximum Quartz frequency	4÷26MHz	4÷16MHz	10÷25MHz	8÷16MHz	8÷16MHz	8÷24MHz
Maximum CPU frequency	168MHz	72MHz	60MHz	16MHz	16MHz	2MHz
Free VIC controller (interrupt)	1	1	1	-	-	-
Programmable I/O (input/output)	140	37	45	32	38	30
PWM (pulse width modulation)	64	12	6	-	-	-
2.4GHz internal ISM modem	-	-	-	-	1	-
Number of contacts	176 LQFP	48 LQFP	64 LQFP	40 PDİP	64 QFN	40 PDİP

The block diagram of the IMD device is given in Fig. 3.

The multifunctional STM32-DC controller is created on the basis of the STM32F103C8T6-BP microcontroller module with a 32-bit ARM-CortexM3 core.

The STM32F103C8T6-BP module is equipped with a CPU central processing unit with a maximum frequency of 72 MHz, 64 KB FLASH, 20 KB SRAM memories, 1-USB2.0 (universal serial bus), 2-SPI (serial peripheral interface), 2-IIC/I2C (inter-integrated circuit), 1-CAN (controller area network) and 3-UART (universal asynchronous reception and transmission) communication and SWD (serial wire debug) serial programming interfaces, 3-internal TIM (timer), RTC (real-time clock) and WDT (watchdog timer) control counters, dedicated peripherals such as 12-bit 10-ADC (analog-to-digital converter), 12-PWM (pulse-width modulation) outputs, 37-I/O input/outputs, and a free VIC (vectored interrupt controller).

The internal controller and peripheral nodes of the multilayer, open-bus architecture STM32 interact freely with each other. Since it is equipped with a free vectored interrupt controller, interrupt functions are performed very quickly and without interfering with other operations.

The system controller of STM32's ARM-CortexM3 core can increase its internal operating frequency up to 72MHz relative to the external quartz frequency of 4MHz÷16MHz and perform 72 MIPS (**m**illion **i**nstructions **p**er **s**econd), i.e., 72 million operations per second [8, 9].

Intelligent devices use various mathematical operations in data processing and calculations. Compared microprocessors also differ in the type, complexity and number of stages of mathematical operations.

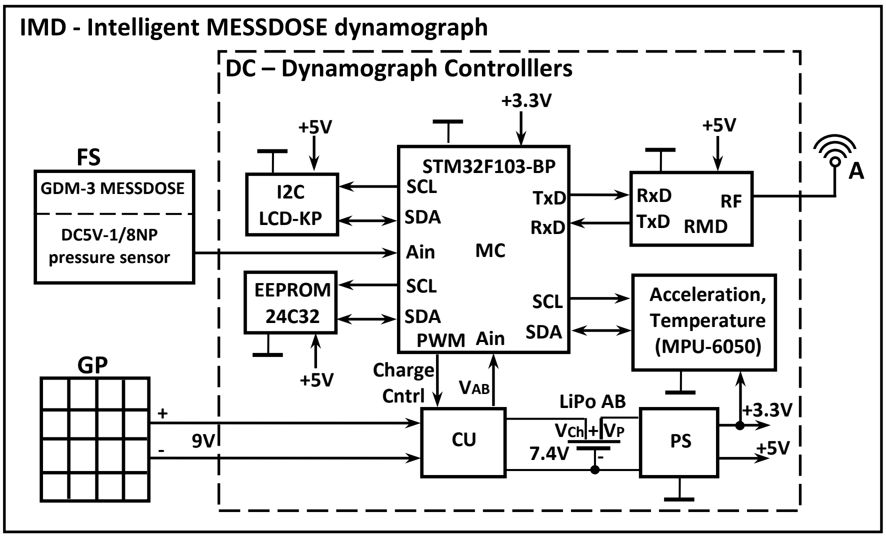

Fig. 3. Block diagram of the intelligent MESSDOSE dynamograph

MCs with MCS-51 and AVR cores perform simple operations only on integers such as addition, subtraction, multiplication and division. And in MC with ARM core, all mathematical operations (addition, subtraction, multiplication, division, raising to square, taking square root, raising to cube, taking cube root, obtaining absolute value, finding remainder, division into integer and fractional parts, rounding, finding the maximum and minimum of two expressions), calculating the exponent, trigonometric functions (sine, cosine, tangent, arcsine, arccosine, arctangent), logarithmic functions (natural logarithm, base 10 logarithm), etc. performed at great speed [10].

ARM-Cortex-M3/M4 processors have cores with different profiles: Cortex-A (application) – intensive application cores that support virtual memory system architecture and are responsible for managing all memory operations; Cortex-M (microcontroller) – microcontroller cores designed for integration into field-programmable devices that perform fast interrupt processing by supporting interrupt programs written in high-level languages; Cortex-R (real-time) – real-time cores that process large volumes of data very quickly.

ARM processors have embedded coders for high performance operations.

Embedded Coder generates and converts MATLAB codes compiled with C++ coder and executes them on ARM processors: easily configures mathematical operations and functions, manages software interfaces, optimizes execution performance, minimizes memory consumption and uses a real-time operating system (RTOS) [11].

Embedded Coder enables ARM processors to function as a complete system within a small chip [12].

Due to its fast operating system, many alternative functions, fast analog and digital inputs and outputs, high buffer capacity, low power consumption, etc., STM32 controller modules become an indispensable work tool widely used in communication and protocol converters, measurement and control devices, modems, voice recognition devices and so on.

The STM32F103C8T6-BP module is a STAMP board mounted on the BASE controller board of the IMD with 40-pin connectors. The module consists of an 8 MHz controller, a 32768 Hz RTC (**r**eal **t**ime **c**lock) real-time quartz, a RST (reset) button, a USB communication port, a SWD programming port, BOOT-0 and BOOT-1 (Boot loader) jumpers for selection of memory sector for loading and running the program, a 40-pin connector for connecting to the BASE module, a Test Led diode, and a +3.3V power supply source, assembled on a 22.5x53mm double-sided PCB (**p**rinted **c**ircuit **b**oard).

The appearance and dimensions of the STAMP circuit board are given in Fig. 4.

The function of the BASE module is to connect the STAMP microcontroller module with peripherals: RF transmitter module, MPU-6050 accelerometer, Atmel-24C32 EEPROM (Electrically Erasable Programmable Read-Only Memory), LCD module with I2C serial interface, keypad, RS232 / RS485 ports, power supply, solar panel, charging unit, etc.

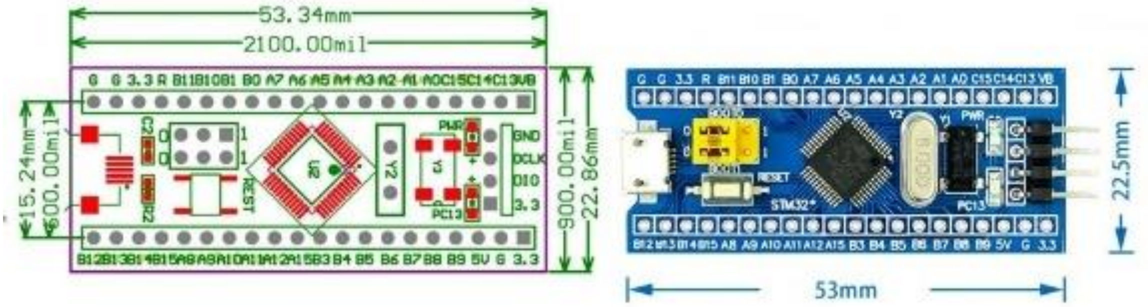

Fig. 4. STM32F103C8T6-BP module and its dimensions

Programming of the STM32F103C8T6-BP STAMP module. Configuration of STM32 Controllers and creation of a working project is performed with STM32CubeMX code generator running in the WINDOWS environment.

The software of the ARM-core STM32 controller is created on PC with KEIL development tools using C++ coder. The C++ file is added to the project to compile the code. A HEX file is created from the C++ codes compiled with KEIL and uploaded to the STM32 controller.

KEIL development tool allows one to create a project without hardware and correct program errors, to simulate output ports without a microcontroller board in debug mode.

STM32CubeMX and KEIL software can be downloaded to the computer from the Internet.

The function of the **RF radiofrequency module** is to exchange data between the IMD and other controller modules or PC. The RF module is built on a 24.4x37.5x4.2mm F8L10A(C)-N transmitter working within a frequency of 410MHz ÷ 441MHz [13, 14].

The appearance of the RF module is given in Fig. 5:

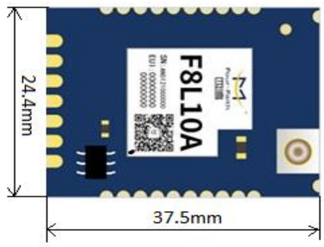

Fig. 5. RF module

MPU-6050 consists of a micro-electro-mechanical system (MEMS) with built-in 3-axis accelerometer, 3-axis compass and temperature sensors. MPU-6050 is a small 14x21mm module with a serial I2C interface that allows measuring the acceleration, velocity, orientation, displacement and temperature of any object [15, 16]. Its appearance is given in Fig. 6.

The MPU-6050 has seven 16-bit ADCs: three 16-bit ADCs for the gyroscope (compass), three 16-bit ADCs for the accelerometer (acceleration), and one 16-bit ADC for digitizing the temperature outputs. For precision tracking of both fast and slow motions, the parts feature a user-programmable gyroscope full-scale range of ±250, ±500, ±1000, and ±2000 °/sec, and a user-programmable accelerometer full-scale range of ±2g, ±4g, ±8g, and ±16g. The output of the temperature sensor (-40°C÷+85°C) varies linearly with an accuracy of ±1°C in the measuring range.

During the movement of the beam, based on the value of the movement speed measured by the MPU-6050 in the IMD device, the moments when the rod passes through the lower and upper dead points are recorded and the period of swing of the beam is determined. Based on the temperature instructions received from the MPU-6050 module, the values of the force sensor are adjusted.

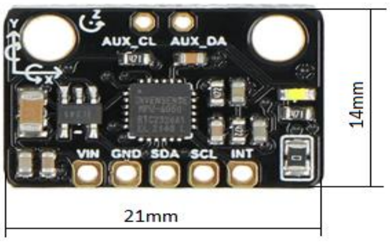

Fig. 6. MPU-6050 module

EEPROM, electrically erasable programmable read-only memory, is a user-modifiable ROM. It can be erased and reprogrammed (written to) repeatedly by applying an electrical voltage.

Atmel-24C32 EEPROM memory element with I2C interface with 32KB capacity was used in IMD. Its function is to remember constant parameters used during device calibration and error correction [17].

LCD with I2C interface is an easy-to-use display module. Its integration with I2C allows the user to easily display complex graphics and text on the LCD screen.

IMD uses a 2-line (16x2=32 characters) I2C LCD1602 liquid crystal display with 16 characters per line [18, 19]. The overall dimensions of the LCD are 38x80mm, its appearance is given in Fig. 7.

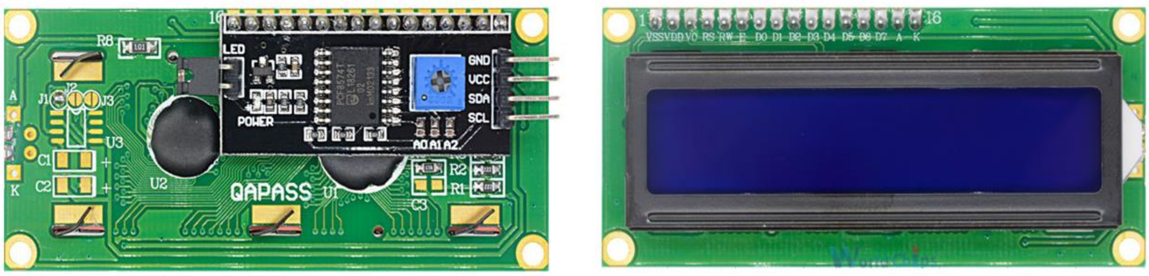

Fig. 7. Front and back view of the I2C LCD-1602 display

Keypad (KP) was added to the LCD screen to select, change, or enter the appropriate parameter in the menu during the sensor calibration. During calibration or during the work process, the selection of the parameter whose value is dynamically controlled on the screen is carried out through KP. A joint view of LCD and KP is shown in Fig. 8.

Fig. 8. LCD and Keypad

The IMD device has RS232 and RS485 ports. Their function is to connect the device to the computer and other microcontrollers.

Power supply source (PS) provides the necessary voltages for the nodes of the IMD. Since the IMD requires little power, it can be powered for a long time by a +7.4V, 3000mAs Lithium Polymer (LiPo) accumulator battery (AB). The voltage of the +7.4V LiPo battery is converted to +5V by the L7805 stabilizer and by AMS1117-3.3 to +3.3V DC, feeding the nodes of the IMD. The battery must be replaced with a new one when its capacity is exhausted. If the LiPo battery is powered by the solar panel, it will not need to be replaced and the IMD can be operated without stopping for a long time.

Charging Unit (CU) ensures healthy charging of the LiPo battery from the Solar panel by adjusting the duty cycle (D%) of the pulse using the pulse width modulation (PWM) method. Based on the charging algorithm, the controller module measures the solar panel and battery voltages and compares them with the lower/upper setpoints. According to the value of the voltages and the comparison results, it decides how to charge the battery.

The diagram of the battery charging algorithm is given in Fig. 9.

According to the algorithm, the CU performs the following functions:

1. When the battery is fully charged, ((V1 > V2) & (SP1 ≤ V2)) prevents the battery from overcharging by limiting the power supplied to the battery by the solar panel (D = 0%);

2. When the battery reaches a fully discharged state, (V2 ≤ SP2) by increasing the power supply to the battery by the solar panel, it ensures the battery is fully charged (D = 100%);

3. When the battery voltage is between the lower and upper setpoints (SP2 < V2 ≤ SP1), based on the difference (Error = V2 – SP1), the value of the error limit (E.l) is calculated: if (E.l < 0), the battery is fully charged with a duty cycle of (D = 100%), if (E.l > 100), the battery charging is stopped with the duty cycle (D = 0%), and if (0 ≤ E.l ≤ 100), the battery is partially (healthy) charged with the duty cycle (D = (E.l * 255) / 100%)).

4. By controlling the temperature of the battery, it is possible to regulate the charging of the battery.

CU's voltages and temperature sensors

1. Voltage sensor:

The dividers used to measure the solar panel and battery voltages each consist of two resistors with R1 (R3) = 100 kOm and R2 (R4) = 20 kOm. The measurement voltage from the common point of R1 and R2 is connected to analog inputs Ain1, and from the common point of R3 and R4 to Ain2 analog inputs of the controller. By controlling the voltages, the controller determines the charging mode of the battery.

2. Temperature sensor:

To measure the battery temperature, the measurement output of the LM35 temperature sensor is connected to the analog input Ain3 of the controller. By controlling the temperature, the controller can adjust the battery charging speed and limit as required.

The chemical reactions of the battery change with temperature. Gassing increases as the battery heats up. As the battery cools, it becomes more resistant to charging. It is important to adjust the charging depending on how much the battery temperature changes. As the temperature increases, the charging limit should decrease.

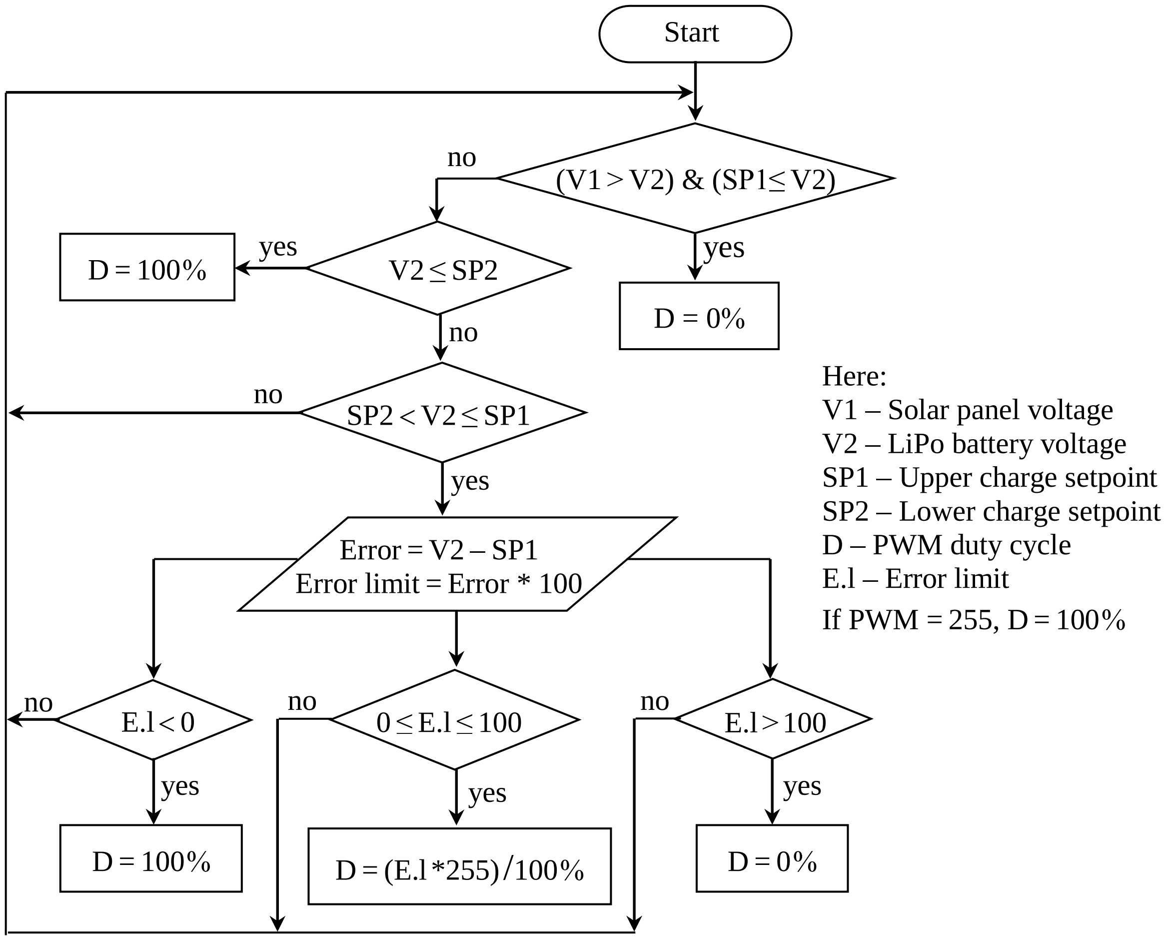

Fig. 9. Charging algorithm of the battery

Calibration of the MESSDOSE load cell

Since the IMD device is a measuring device, it must be calibrated from time to time. The calibration process is performed with the help of a specially designed compression device (CD).

The CD consists of a specially designed body that can withstand 8 tons of weight, two plates moving along the arms of the body, and a compressing mechanism [20].

The connection diagram of test measurement equipment for calibration is given in Fig. 10:

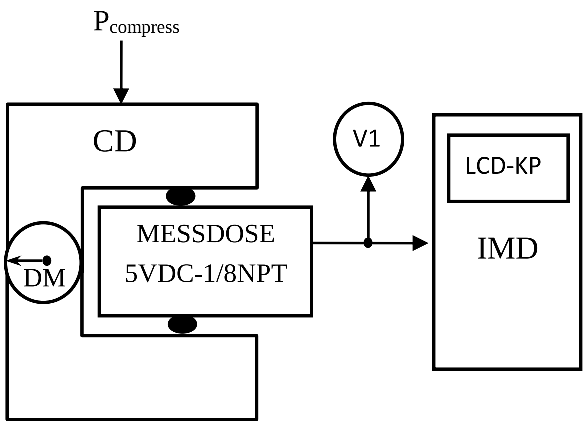

Here:
CD – Compression device;
$P_{compress}$ – value of the compression force produced by the compression device;
DM – dynamometer showing the compression force;
MESSDOSE – load cell;
V1 – Multimeter monitoring output voltage of 5VDC-1/8NPT pressure sensor;
IMD – Intelligent MESSDOSE dynamograph;
LCD-KP – Liquid crystal display and keypad.

Fig. 10. Test measurement equipment

The body of the 5VDC-1/8NPT pressure sensor, which is the sensitive element of the MESSDOSE force transducer, is made of stainless metal, it works with a voltage of 5VDC, the output signal varies in the range of 0.5V÷4.5V; the output voltage at zero pressure along the selected measuring range = 0.5V, the output voltage at half of the pressure range = 2.5 V and at maximum pressure the output voltage varies linearly at = 4.5V. It has full scale accuracy +/-0.5%, operating temperature -40 ÷ +120°C, protection class IP67, impact response time ≤ 1ms, insulation resistance >100mΩ 500VDC, explosion resistance class ExiaTTCT6, electromagnetic compatibility EN50051-1.

In the SI International System of Units, 1 Newton (N) is taken as the unit of force that gives 1 kilogram of mass an acceleration of 1 meter per second.

Usually, the unit of measurement of a pressure sensor is expressed in "psi" lbf/in^2 (pounds per square inch) or "bar", and the load on the hanger of the beam is expressed in "Newtons" or "tons".

Approximate conversion rules for various measurement units are given in Table 2 below.

Table 2

Conversion factors of measurement units

Unit	**Symbol**	**Equivalency**
1 pound	lb	0.45359237 kg
1 pound-force	lbf	4.44822 N
1 kilogram-force, kilopond	kgf (kp)	9.80665 N
1 ton-force	tonf	9806.65 N
1 pound-force	lbf	4.44822 N
1 newton/square meter	N/m^2	0.0001450377 psi
1 psi (pounds per square inch)	lbf/in^2	6894.76 N/m^2
1 psi (pounds per square inch)	lbf/in^2	144 lbf/ft^2
1 foot	ft	12″ (inch)
1 bar	bar	0.98692326671 atm
1 bar	bar	14.503773773 psi
1 bar	bar	100000 N/m^2

Based on the conversions in the table, the equivalent "psi" measurement limit of the pressure sensor selected to determine the value of the compression force acting on a 10 ton load is as follows:

$$10 \text{ tonf} = 98066.5 \text{ N} = 98066.5 * 0.0001450377 \text{ psi} = 14.22334 \text{ psi}.$$

Therefore, a 10 ton load can be determined with an IMD fitted with a 5VDC-1/8NPT pressure sensor operating at a measurement range of 0 ÷ 15psi.

The appearance and output graph of the 15psi/10ton 5VDC-1/8NPT pressure sensor is shown in Fig. 11. As can be seen from the graph, the output voltage value of the sensor designed for a maximum pressure of 15psi varies linearly with = 0.5V at 0.0psi pressure, = 2.5V at 7.5psi and = 4.5V at 15psi.

Thus, when using such a pressure sensor, the output measuring signal, regardless of the load, changes according to a regular linear law, and the accuracy coefficient is high, which minimizes the error in the dynamograph chart.

When the MESSDOSE load cell is compressed between the plates of the CD with a $P_{compress}$ force, a voltage corresponding to that force is generated at the output of the 5VDC-1/8NPT pressure sensor and enters the Ain1 analog input of the IMD device. The dynamometer DM on the CD shows the values of the input $P_{compress}$ force, and the multimeter V1 connected to the sensor output shows the values of the measured voltage.

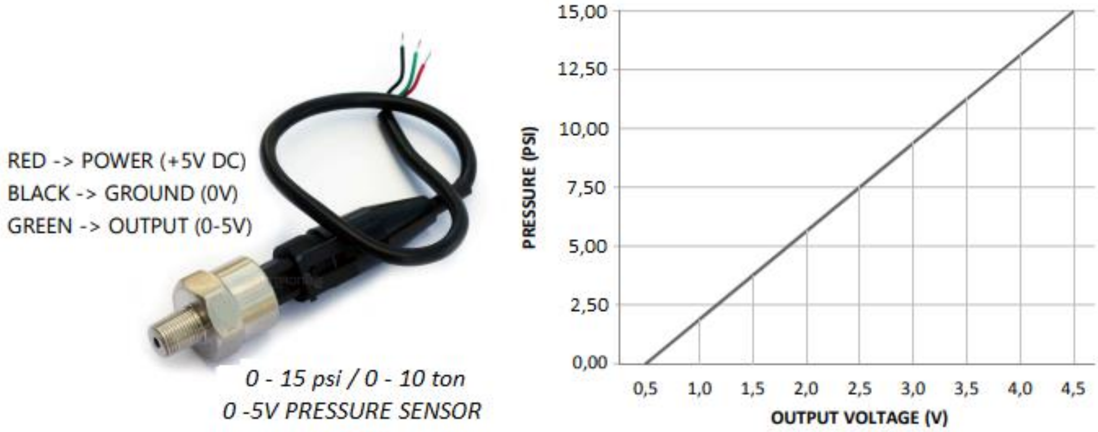

Fig. 11. Appearance and output graph of the 15psi/10ton 5VDC-1/8NPT pressure sensor

The function of the pressure sensor is to provide an analog output signal corresponding to a static or inertially varying compression-release force.

The pressure sensor fulfills its metrological characteristics when operating at -50°C ÷ +50°C temperature, 630 ÷ 800 mm of mercury atmospheric pressure and 5VDC supply voltage.

After connecting the MESSDOSE pressure transmitter to the supply voltage, it is necessary to wait 15 minutes, so that a stable temperature regime is established due to the current flowing through the sensitive elements.

Before calibration, the MESSDOSE dynamograph should be loaded three times with maximum force. The application time of each load should be up to 1 ÷ 1.5 minutes. At least 30 seconds after the load is completely removed, the indication corresponding to the absence of force (P_0) should be recorded.

Then, in order to calibrate the device within the limit ($P_0 \div P_{max}$), the loading points corresponding to the known input $P_{compress}$ force of the sensor must be predetermined. Measurements should be done in three stages and there should be an interval of at least three minutes between stages. At each stage, the loading should be carried out at the same measurement points (i) in the loading - release process, first changing from P_0 to P_{max} and then from P_{max} to P_0. $U_{average}$ values of the measured output voltages of the sensor corresponding to the $P_{compress}$ force are determined at the same points of the three stages.

The rating characteristic of the force sensor, i.e., the graph of the slope between the output voltage and the input $P_{compress}$ force, is determined experimentally, and a table is drawn up based on the results of the measurement. The rating characteristic is established based on the corresponding $P_{compress}$ and $U_{average}$ values.

Assume that the $P_{compress}$ force was measured three times at point (i) and their values were different: U_y1, U_y2, U_y3 (loading) and U_b1, U_b2, U_b3 (release). Variation (V_i) at the considered measurement point (i) is determined by the modulus of the difference of the average values in loading and release modes.

$$\mathrm{Vi} = \left| \frac{Ub1 + Ub2 + Ub3}{3} - \frac{\mathrm{Uy1} + \mathrm{Uy2} + \mathrm{Uy3}}{3} \right|$$

The Hysteresis error at the considered measurement point (i) is determined by the maximum value of the Variation as follows:

$$H = \pm \frac{max(Vi)}{2}$$

4. Conclusion

By combining the traditional GDM-3 "MESSDOSE" dynamograph with multifunctional DC in a single housing, a modern alternative energy-powered IMD fitted with force, acceleration (displacement) and temperature sensors, a calibration feature, display and keypad, radio frequency connection, which can be easily installed between the crossheads of SRPU, has been created.

Compared to traditional dynamographs and load cells, the IMD device has many advantages:

1. Since the measuring sensors are in the same housing as the IMD device, there is no need for a connecting cable and the useful signals are not distorted;
2. The IMD device wirelessly transmits measurement data to the well controller;
3. The presence of a special calibration algorithm and an LCD-KP display-keypad panel allows the IMD to work as a "Calibration Device" during the calibration of the force transmitter;
4. The IMD is powered by a rechargeable battery that is charged from an alternative energy source – a solar panel – and has an automatic charging unit to ensure uninterrupted power;
5. Force (5VDC-1/8NPT) and displacement (MPU-6050) sensors with standard output and accurate specifications allow for more accurate dynamometer charts;
6. Placing all components of the IMD device in a single housing results in the simplification of the electrical circuit and increased reliability;
7. The large memory of the dynamograph controllers DC built on the basis of STM32 microprocessor allows for transmitting dynamometry data both point-by-point in real time and all point data during a full cycle by collecting all point data in the memory and transferring them at once, etc.

References

[1] A.X. Mirzəcanzadə, M.Ə. İskəndərov, M.Ə. Abdullayev, R.Q. Ağayev, S.M. Əliyev, Ə.C. Əmirov, Ə.F. Qasımov, “Neft və qaz yataqlarının istismarı və işlənilməsi”, Baku, (1960) 444 p. [In Azerbaijani: A.Kh. Mirzajanzade, M.A. Iskanderov, M.A. Abdullayev, R.G. Agaev, S.M. Aliev, A.J. Amirov, A.F. Gasymov, Operation and Development of Oil and Gas Fields].

[2] V.T. Məmmədov, O.H. Mirzəyev, “Neft mədən texnikasinin təmiri və bərpasi”, Baku, (2012) 285 p. [In Azerbaijani: V.T. Mammadov, O.H. Mirzayev, Repair and Restoration of Oil Field Equipment].

[3] Ə.H. Əzizov, M.A. Qarayev, H.Ə. Heydərov, S.Ə. Ağammədova, “Həcmi hidravlik maşinlar”, Baku, (2010) 601 p. [In Azerbaijani: A.H. Azizov, M.A. Garayev, G.A. Heydarov, S.A. Agammadova, Volumetric Hydraulic Machines].

[4] К.Р. Уразаков, В.В. Андреев, В.П. Жулаев, “Нефтепромысловое оборудование для кустовых скважин”, Москва, Недра. (1999) pp.80-81. [In Russian: K.R. Urazakov, V.V. Andreyev, V.P. Zhulayev, Oil Field Equipment for Cluster Wells, Moscow, Nedra].

[5] Ас.Г. Рзаев, “Интеллектуальный межтраверсный датчик усилия”. [In Russian: As.G. Rzayev, Intelligent Inter-Crosshead Force Sensor].

[6] Y.G. Aliyev, Modernized MESSDOSE intelligent force sensor, Informatics and Control Problems. 42 No.2 (2022) journal homepage: www.icp.az

[7] В.В. Андреев, К.Р. Уразаков, В.У. Далимов и др., “Справочник по добыче нефти”, под ред. К.Р. Уразакова, Москва, ООО “Недра-Бизнесцентр”, (2000) 374 p. [In Russian: V.V. Andreyev, K.R. Urazakov, V.U. Dalimov, et al, Oil Production Handbook, ed. by K.R. Urazakov, Moscow, Nedra-Business-Center LLC].

[8] RM0008 Reference manual STM32F101xx, STM32F102xx, STM32F103xx, STM32F105xx and STM32F107xx advanced Arm-based 32-bit MCUs.

[9] STM32F103C8T6 - Blue Pill Development Board
https://components101.com/microcontrollers/stm32f103c8t8-blue-pill-development-board

[10] https://www.javatpoint.com “C++ Math Functions”.

[11] https://www.mathworks.com/hardware-support/arm.html “ARM Support from Embedded Coder”.

[12] "ARM Processors: Embedded CPUs" – Ryerson University.

[13] F8L10C-10, F8L10-10E LoRa Module Technical Specification V2.0.0

[14] F8L10C Series LoRa Module User Manual V1.0.0

[15] MPU-6000 and MPU-6050 Product Specification Revision 3.4, https://invensense.tdk.com/wp-content/uploads/2015/02/MPU-6000-Datasheet1.pdf

[16] MPU-6000 and MPU-6050 Register Map and Descriptions Revision 4.2, https://invensense.tdk.com/wp-content/uploads/2015/02/MPU-6000-Register-Map1.pdf

[17] 2-Wire Serial EEPROM AT24C32-64 / https://ww1.microchip.com/downloads/en/DeviceDoc/doc0336.pdf

[18] I2C Serial Interface 1602 LCD Module, http://www.handsontec.com/dataspecs/module/I2C-1602 LCD.pdf

[19] 1602A-1 LCD Module Specification Ver1.0, https://www.openhacks.com/uploadsproductos/eone-1602a1.pdf

[20] As.H. Rzayev, Y.Q. Əliyev, M.H. Rezvan, Sıxıcı dərəcələmə stendinin yaradılması, Riyaziyyatın tətbiqi məsələləri və yeni informasiya texnologiyaları, 3-cü Respublika elmi konfransı, SDU, Sumqayit, December 2016, pp.231-232. [In Azerbaijani: As.H. Rzaev, Y.G. Aliyev, M.H. Rezvan, Development of compression estimation bench, Applied Problems of Mathematics and New Information Technologies, 3rd Republican Scientific Conference]